Secondary structure of cell-penetrating peptides controls membrane interaction and insertion.

Emelía Eiríksdóttir, Karidia Konate, Ulo Langel, Gilles Divita, Sébastien Deshayes

Secondary Structure of Cell-Penetrating Peptides Controls Membrane Interaction and Insertion

Emelía Eiríksdóttir [a*], Karidia Konate [b*], Ülo Langel [a,c], Gilles Divita [b,d], Sébastien Deshayes [b]

[a] Department of Neurochemistry, Stockholm University, S-106 91 Stockholm, Sweden.

[b] Centre de Recherches de Biochimie Macromoléculaire, CRBM-CNRS, UMR-5237, UM1-UM2, University of Montpellier, Department of Molecular Biophysics and Therapeutics, 1919 Route de Mende, 34293 Montpellier, France.

[c] Laboratory of Molecular Technology, Institute of Technology, University of Tartu, 50411 Tartu, Estonia.

* These authors contributed equally to this work.

[d] To whom correspondence should be addressed; tel : +33 (0)4 67 61 33 92, fax : +33 (0)4 67 52 15 59, e-mail : gilles.divita@crbm.cnrs.fr

Abstract

The clinical use of efficient therapeutic agents is often limited by the poor permeability of the biological membranes. In order to enhance their cell delivery, short amphipathic peptides called cell-penetrating peptides (CPPs) have been intensively developed for the last two decades. CPPs are based either on protein transduction domains, model peptide or chimeric constructs and have been used to deliver cargoes into cells through either covalent or non-covalent strategies. Although several parameters are simultaneously involved in their internalization mechanism, recent focuses on CPPs suggested that structural properties and interactions with membrane phospholipids could play a major role in the cellular uptake mechanism. In the present work, we report a comparative analysis of the structural plasticity of 10 well-known CPPs as well as their ability to interact with phospholipid membranes. We propose a new classification of CPPs based on their structural properties, affinity for phospholipids and internalization pathways already reported in the literature.

Keywords: Cell-penetrating peptides, structure, membrane interactions, conformation, versatility.

1. Introduction

Development of new therapeutics broadly increased during the last years. The enhancement of the knowledge of the human genome and its corresponding proteomes and interactomes led to innovative strategies in the design and improvement of bioactive molecules. However, although these bioactive agents have shown a strong efficiency and attractive activities, their cellular internalization still remains the main limitation for their clinical use. Biological membranes are often pointed out as the first reason of the encountered cellular delivery troubles because they generally constitute impermeable barriers for drugs. Several delivery systems have been conceived in order to overcome the low permeability of nuclear or plasma membranes and various methods have aimed to improve therapeutics delivery, such as viruses and liposomes. Among them are carrier peptides called cell-penetrating peptides (CPPs) which have undergone a strong development during the last twenty years [1]. CPPs are generally described as short amphipathic or purely cationic peptides of less than 30 amino acids which possess a positive net charge, are able to penetrate biological membranes and transfer covalently or non-covalently attached bioactive cargoes into cells [2]. More than 20 different CPPs have been described so far and were applied for the delivery of various cargoes. From small particles to peptides, proteins and nucleic acids, the CPP-mediated internalization of a cargo has been validated into a wide variety of cell types from different tissues and organisms [3,4]. Although the efficiency of CPPs has clearly been proved, their mode of action still remains puzzling. Early on, direct translocation [5-8], endocytotic processes [9-12] or combination of several mechanisms [13] were suggested as possible delivery pathways for CPPs. Nowadays, the most plausible explanation for the mechanism of cellular entry seems to be a complex combination of several parameters. Understanding the cellular uptake mechanism of CPPs constitutes a crucial factor to decipher, in order to determine the intracellular behavior and efficiency of the cargo. Several

approaches have been undertaken to identify the different parameters involved in the cellular uptake. The structural properties as well as the interaction with membrane components such as heparan sulfate or lipid-raft domains have been studied [11,14,15]. However, although some similar features exist between the most efficient CPPs, no clear rules can be proposed.

In the present work, we have compared the alteration in structural state and the interaction of 10 CPPs with model membranes, in order to classify the CPPs with regard to both their biophysical properties and their ability to enter the cell. CPPs are usually divided into three classes; protein transduction domains (PTDs), model peptides and designed peptides, as shown in Table 1. PTD peptides are natural peptides derived from specific protein fragments with transduction abilities. This class contains the Tat-peptide corresponding to the 48-60 segment of the transactivator TAT protein of the HIV-1 virus [16], the Penetratin derived from the third helix of the Antennapedia homeodomain (segment 43-58) [17], EB1 where certain residues of Penetratin have been substituted by histidine [18], pVEC and retro-pVEC variant derived from the murine cell adhesion molecule vascular endothelial cadherin [19], and M918 and its M1073 variant derived from the tumor suppressor protein p14ARF (amino acids 1-22) [20]. Model peptides consist of amino-acid sequences that are generally based on repeat motifs or poly-residues, such as MAP and polyarginines [21,22]. Designed peptides have been conceived on the basis of rational mutations or combinations between protein domains of a specific interest. TP10 is a truncated form of Transportan that associates a neuropeptide with a segment derived from wasp venom [23]. MPG, MPG-α and Pep-1 combine a fusion peptide or a tryptophan-rich segment with a nuclear localization sequence [24-26]. Finally, CADY consists of a variant of the fusion peptide JTS1 [27].

In the present work, we have investigated both the structural state and the conformational plasticity of peptides in several distinct environments. The structural flexibility of each peptide has been evaluated by circular dichroism (CD) spectroscopy. The

amphipathic character for all carriers as well as their affinity for different phospholipids monolayer have been determined by surface physic methods. Taken together these results enable us to identify three classes of CPPs and to select four peptides that display common features with the well-known MPG, Pep-1 and CADY peptides [25-28]. The structural and binding results were combined with the cellular uptake investigations from the literature.

2. Materials and methods

2.1. Reagents.

t-Boc-protected amino acids were purchased from Neosystem (Strasbourg, France) and Iris Biotech (Marktredwitz, Germany). 1-hydroxybenzotriazole, *N,N'*-diisopropylethylamine, *N,N'*-dicyclohexylcarbodiimide and 4-methylbenzhydrylamine-polystyrene resin were purchased from Iris Biotech (Marktredwitz, Germany) while *N,N'*-dimethylformamide from Fluka Chemie GmbH (Buchs, Switzerland). 8-aminonaphtalene-1,3,6-trisulfonic acid (ANTS) and his quencher p-xylene-bis-pyridinium bromide (DPX) were purchased from Invitrogen (Cergy Pontoise, France).

2.2. Peptides synthesis.

The peptides were synthesized in a stepwise manner on an automated peptide synthesizer (Applied Biosystems model 433A, USA) by *tert*-butoxycarbonyl (*t*-Boc) chemistry. *t*-Boc amino acids were coupled as 1-hydroxybenzotriazole (HOBt) esters in the presence of *N,N'*-dicyclohexylcarbodiimide and *N,N'*-diisopropylethylamine on 4-methylbenzhydrylamine resin to generate *C*-terminally amidated peptides.

Peptides containing His(Dnp) or Trp(For) were deprotected with 20 % thiophenol in DMF for 1 h or 20 % piperidine in DMF for 1 h, respectively. Cysteine- or methionine-containing peptides were cleaved from the resin in hydrogen fluoride (HF)/*p*-cresol/*p*-thiocresol (90/5/5) for 1 h at 4°C, extracted with 10% aqueous acetic acid and washed with diethylether; all other peptides were cleaved in HF/*p*-cresol (90/10). Finally, the peptides were purified by semi-preparative reverse-phase HPLC column (Discovery®BIO Wide Pore C-18, Supelco®, Sigma-Aldrich, MO, USA), and their purity checked by RP-HPLC analytical column (Discovery® C-18, Supelco®). The correct molecular weight was verified by Perkin Elmer prOTOF™ 2000 MALDI-TOF (Perkin Elmer, Sweden) mass spectrometry.

2.3. Phospholipids.

Dioleoylphosphatidylcholine (DOPC) and dioleoylphosphatidylglycerol (DOPG) were purchased from Avanti Polar Lipids (Alabaster, AL, USA). Sphingomyelin (SM) and cholesterol (Chol) were purchased from Sigma-Aldrich (Saint Louis, MO, USA).

2.4. Small and large unilamellar vesicles

Small Unilamellar Vesicles (SUV) were prepared from DOPC, DOPG or a mixture of DOPC and DOPG (80/20, m/m) by sonication. Phospholipid powder was dissolved in a chloroform/methanol mixture (3/1, v/v). The solvent was evaporated under high vacuum for at least 3 hours to remove residual solvents. The lipids were resuspended in pure water by vortex mixing. The resulting lipid dispersion was sonicated in one cycle (20 min at 70% pulse cycle in an ice/water bath) using a 450D Digital Sonifier (Dietzenbach, Germany). At last, a centrifugation of the resulting vesicles allowed the cleaning of the remaining titanium particles from the sonication probe.

Large Unilamellar Vesicles (LUV) were prepared by the extrusion method from a mixture of DOPC, sphingomyelin and cholesterol (40/40/20, mol/mol/mol). The respective powder were dissolved in a chloroform/methanol mixture (3/1, v/v) and gently mixed. The solvent was evaporated under high vacuum for at least 3 hours to remove residual solvents. The lipids were resuspended in a 5mM phosphate pH 7.5 buffer by vortex mixing. Then 5 freeze-pump-thaw cycles were applied and then LUV were obtained by extrusion through a 0.1 mm polycarbonate membrane (Avanti Polar Lipids, Alabaster, AL, USA). Finally, SUV and LUV preparations were equilibrated overnight at 4°C and used the following day.

2.5. Leakage of liposomes

The release of a substance encapsulated in liposomes is followed by fluorescence using a SPEX-PTI spectrofluorimeter in a 1 cm pathlength quartz cell, with a band-pass of 2 nm for excitation and emission. ANTS and his quencher DPX were both encapsulated in the aqueous phase of liposomes. Liposomes were eluted on a Sephadex G50 to remove free ANTS and DPX from medium. The ANTS fluorescence was measured at room temperature using excitation and emission wavelengths at 355 nm and 512 nm, respectively. The liposome leakage induces the release and dequenching of ANTS. The percentage of release is then defined as Ft/Ftot x100, where Ft is the fluorescence signal at t time and Ftot is the signal obtained after vesicle lysis with 1% Triton X100.

2.6. Circular Dichroism (CD) spectroscopy.

CD spectra were recorded on a Jasco 810 dichrograph in quartz suprasil cells (Hellma) with an optical path of 1mm for peptide in solution or in the presence of small unilamellar vesicles. Same concentrations of peptide were used for each condition. Spectra were obtained from 3 accumulations between 190 and 260 nm with a data pitch of 0.5 nm, a bandwidth of 1 nm and a standard sensitivity.

2.7. Langmuir-Blodgett film balance. - Adsorption at the Air-Water Interface.

Adsorption studies at the air-water interface were carried out using a home made Langmuir trough and the surface tension was measured with a Prolabo tensiometer (Paris, France), using the platinum plate method of Wilhelmy [30]. The surface pressure measurements were made at equilibrium after an injection of a small amount of the peptide-solutions into the subphase, followed by a gentle stirring with a magnetic stirrer. The subphase consists of a NaCl 0.154 M solution. Critical micellar concentration (CMC) was

determined by repeating this procedure until no further increase of the surface pressure could be detected.

2.8. Langmuir-Blodgett film balance. - Penetration into a phospholipid monolayer.

Regarding the penetration measurements of the peptides into the phospholipids, a lipid monolayer was initially obtained by spreading a solution of the lipid in chloroform/methanol (3/1, v/v) onto the air-NaCl aqueous solution interface in order to obtain a defined surface pressure. The solvent was allowed to evaporate and when a constant surface pressure was reached, a small volume of the aqueous peptide solution, close to the CMC, was injected into the subphase beneath the lipid monolayer. Increase of the surface pressure was recorded for different initial lipid surface pressures in order to identify the critical pressure of insertion (CPI) of the peptide into the phospholipid monolayer.

3. Results

Structural properties and the secondary structure of CPPs have recently been reported to control to a certain extent their cellular uptake mechanism and to be associated with a specific route of entry [31]. In the present work, we have investigated the physico-chemical properties of 10 well known and defined CPPs in order to classify them into "biophysical" subgroups. These CPPs (PTDs, model or chimeric peptides) have been successfully used either through covalent or non-covalent strategies for the delivery of bioactive cargos, and have been reported to enter cells via different pathways (Table 1). Additionally, the YDEGE peptide, an 8-residue peptide (YDEEGGGE-NH_2) which in unable to enter cells [20], has been used as a negative control.

3.1. Structural characterization of CPPs in pure water (in their free form)

We first investigated the conformational state of each CPP in its free form by circular dichroism (CD) spectroscopy. As reported in Fig. 1 and Table 2, all the CPPs presented the same CD spectra in a solution characterized by a minimum centered at 198 nm. These results demonstrate that all the analyzed CPPs were random coils in a solution, despite the differences in their nature [32]. Interestingly, the CD spectra of highly charged carriers such as Tat and Arg_9 were similar to the ones of the control YDEGE-peptide, displaying a positive maximum at 217 nm characteristic of a full disordered structure, generally typical for a random coil spectrum (Fig. 1) [32]. In contrast, the CD spectra for Penetratin, TP10, MAP, EB1, pVEC, retro-pVEC, M918 and M1073 did not show a maximum at 217 nm, suggesting the presence of a mixture of structural conformations and a low level of secondary structures. Similar results have also been reported for MPG, MPG-α and CADY peptides [25,29] that are mainly random coils in a solution. Finally, similar CD results were obtained for all the CPP-concentrations used herein (50 - 150 μM), which suggests that aggregation or auto association

of the peptides are not involved. This is in contrast to Pep-1, the only CPP able to adopt a helical structure in pure water at high concentrations (1 mM) [28].

3.2. Structural characterization of peptides in the presence of phospholipids

We then investigated the impact of the presence of model membranes on the structural state of CPPs, by using several distinct types of liposomes (Table 2). The structure of the CPPs was determined by CD in the presence of SUV containing either negatively charged phospholipids (DOPG), neutral phospholipids (DOPC) or a 80/20 mixture of DOPC/DOPG as well as in the presence of LUV composed of a 40/40/20 mixture of DOPC/SM/Chol. The DOPC/DOPG mixture was used in order to identify CPP structures under partially charged conditions. The DOPC/SM/Chol LUVs were used to mimic the composition of more stable and natural plasma membrane. As reported in figure 1A and table 2, analysis of the CD spectra reveals that the CPPs can be classified into three subgroups based on their secondary structure. The first group, involving Tat, Arg_9 and the control peptide, displayed no change in the CD spectra despite the different nature of the phospholipids or the lipid/peptide ratios used (Fig. 1A). Indeed, the corresponding CD spectra in the presence of DOPC, DOPG, DOPC/DOPG SUVs and DOPC/SM/Chol LUVs were similar to those recorded for the peptides alone and characterized by a minimum at 198 nm. These peptides showed a marked structural polymorphism as they remained disordered in all environments tested (Table 2).

The second group corresponds to pVEC, its retro-pVEC analogue, Penetratin, M918 and M1073 peptides which adopted a β-structure in the presence of negatively charged phospholipids DOPG (Table 2, Fig. 1B). For these peptides, increasing the concentration of the phospholipids triggered conformational changes from random coil to β-structure. As reported for M918 in figure 1b, CD spectra in the presence of DOPG were characterized by

low ellipticity values and a maximum centered around 196-198 nm while a single minimum was detected around 219 nm which is typical for β structure spectra [32].

The third group contains TP10, MAP and EB1 peptides that adopted a helical conformational state in the presence of DOPG phospholipids (Table 2). As shown in Fig. 1C, for the EB1 peptide, a structural transition from a disordered structure to a α-helical conformation occurred for a lipid/peptide ratio of 5/1. Indeed, the CD spectra exhibited a maximum centered at 194 nm and two minima at 207 nm and 222 nm, which are in agreement with a main α-helical conformation [32]. Taking into account the intensity of the band at 222 nm (around 12500), it clearly appears that the helical domain does not involve all the sequence but probably few residues (a third of the sequence). These results emphasize a monomorphic behavior of these CPPs in the presence of DOPG. Moreover, the increase in intensity of the band at 222 nm for high lipid/peptide ratio suggests an increase in helical content. The analysis of the ratio of intensities at 222 and 208 nm can be used to distinguish helix aggregation (ratio ≥1 for coiled coils) from monomeric helices (ratio ≤0.86 for isolated helices) [33,34]. Thus the 222/208 nm ratios indicate that an aggregation of helices probably occurs for all peptides in the presence of fully negatively charged lipids (DOPG) while the ratio in the presence of DOPC/DOPG mixture suggest isolated helices (as for TP10 in Fig. 2B and 2C).

In contrast, in the presence of the DOPC zwiterrionic liposome or DOPC/SM/Chol (40/40/20) LUVs no conformational changes of the CPP were observed (Table 2). The CD spectra for all the CPPs were characterized by a minimum at 198 nm for all the lipid/peptide ratios, indicating a random coil state as reported for TP10 in Fig. 2A and 2D. In the presence of DOPC/DOPG vesicles a significant increase of the α-helical structural contribution was observed. Indeed the CD spectra of TP10, MAP and EB1 underwent a slight change corresponding to a shift of the single minimum at 198 nm to 205 nm associated with a

minimum at 220 nm and a maximum around 190 nm (Fig. 2B). In contrast, no modification in the structure of pVEC, retro-pVEC, M918 or Penetratin was observed in the mixed vesicles suggesting that electrostatic interactions play a major role in the folding of these peptides and that only 20% of DOPG in the vesicles is not enough to stabilize the beta structure. With regard to the CD spectra recorded in LUVs, the presence of sphingomyelin, cholesterol and phosphate buffer led to similar CD profiles to those obtained with pure DOPC SUVs, except for CADY that displays a helical conformational transition (Table 2). Taken together, the CD analyses in DOPC, DOPG, DOPC/DOPG SUVs and DOPC/SM/Chol LUVs suggest that the lipid-mediated CPP conformational transitions are mainly dependent on electrostatic interactions, i.e. charges effect.

3.3. Affinity of the CPP for air-water interface by adsorption experiments

Air-water interface constitutes a useful model to investigate the affinity of the peptides for a hydrophobic/hydrophilic interface [35]. We have therefore performed adsorption experiments in order to determine the interfacial properties and amphipathicity of the different CPPs [30]. The interfacial properties and the affinities for a lipid-free air-water interface of Arg_9, Tat, pVEC, Penetratin, M918, EB1, TP10 and MAP were evaluated by measuring the variation of the surface tension as a function of the peptide concentration in the subphase (Fig. 3). Saturation of the surface pressure was reached for TP10, MAP, EB1 and M918, but not for Arg_9, Tat, Penetratin and pVEC. The corresponding saturating surface pressure (π_{sat}) values for EB1 (10 mN/m), MAP (14 mN/m) and TP10 (20 mN/m) are quite similar to those already described for MPG and MPG-α [25], suggesting that these peptides display a clear amphipathic character (Table 3). The π_{sat} value obtained for M918 (7 mN/m) is more related to that observed for Pep-1 [28] corresponding to a less amphipathic character. However, the π_{sat} values obtained for these CPPs are rather low compared to the 30 mN/m recently

identified for the strong amphipathic CADY peptide [29]. Critical micellar concentration (CMC) was determined for each peptide from variation of their induced surface pressure and is 38 nM, 59 nM, 91 nM and 130 nM for TP10, MAP, EB1 and M918, respectively (Table 3). These values are rather low in comparison to MPG, Pep-1 and CADY (250, 400, 500 nM) [25,28,29]. In contrast, the addition of up to 1 μM Arg_9, Tat, Penetratin and pVEC in the subphase did not induce any significant increase in the surface pressure, suggesting that these peptides are poorly amphipathic (Fig. 3). When the CMC and π_{sat} values are taken together, peptides of the "beta-sheet" and "helix" groups can be ranked regarding to their amphipathic character. The results clearly show that the "helix" peptides are more amphipathic (with the following order TP10>MAP>EB1) than the "beta-sheet" peptides, with only M918 exhibiting a weak amphipathic nature. Arg_9, Tat, Penetratin and pVEC did not display any interfacial properties.

3.4. Affinity of the CPPs for phospholipid monolayer by penetration measurements

The affinity of the peptides for phospholipids and their ability to insert into phospholipid films spread at the air-water interface were measured by monitoring the variation in surface tension and by using different initial pressures associated with an injection of the peptides in the subphase. [30,36]. The peptide concentration used here was slightly lower than its CMC [37]. Critical pressures of insertion (CPI) were then determined by extrapolation of the initial surface pressure for a variation of surface pressure equal to zero (πi for $\Delta\pi=0$). As for the CD analysis, we have compared two types of lipid monolayers, i.e. negatively charged phospholipids (DOPG) and neutral phospholipids (DOPC). Since Arg_9, Tat, Penetratin and pVEC presented no interfacial properties, we focused on the TP10, MAP, EB1, M918 peptides and the results were compared to the previously analyzed CPPs MPG, Pep-1 and CADY (Table 3).

The CPI values for EB1, TP10 and MAP were estimated to be around 30 mN/m (33, 31 and 28 mN/m, respectively) for DOPC monolayer, suggesting that these peptides are able to insert spontaneously into the phospholipid monolayer and into biological membranes (CPI values > 30-35m/M) [36,38] (Table 3, Fig. 4). Their affinity for the lipid film is close to that of MPG and MPG-α (33mN/m) but rather lower compared to CADY and Pep-1 (43 and 45mN/m, respectively). The CPI value obtained for M918 in DOPC is lower (23 mN/m) than for the other CPPs [25,28,29], indicating a weaker insertion of this peptide into the DOPC monolayer as already suggested by the CD experiments. In addition, information on interactions between the peptides and the phospholipids can be evaluated by extrapolation of the variation of the surface pressure at zero initial pressure ($\Delta\pi$ for $\pi i=0$) where surface pressures higher than the peptides π_{sat} generally suggest strong peptide-lipid interactions [30]. In the case of the DOPC monolayers, the extrapolated values are quite similar to π_{sat} for all the peptides except for EB1 that displays a little deviation around 4mN/m from π_{sat} (Fig. 4). These observations indicate that the "helix" peptides are able to insert into the monolayer of the neutral phospholipid DOPC with weak interactions while M918 is not. The order of interaction is EB1>TP10>MAP.

In contrast, all the evaluated peptide showed a better affinity for the DOPG monolayers, with extrapolated CPI values higher than 40 mN/m, clearly indicating a better insertion of all peptides in this monolayer compared to DOPC (Table 3, Fig. 5). Furthermore, these high CPI values suggest that the peptides can spontaneously insert into natural membranes (CPI values > 30-35m/M) [36,38]. Interestingly, M918 strongly interacts with the negatively charged phospholipids with a high CPI value of 78 mN/m extrapolated for $\Delta\pi=0$ and a variation of surface pressure at zero initial pressure ($\Delta\pi$ for $\pi i=0$) of 15 mN/m. This is twice the π_{sat} value, suggesting strong peptide/lipid interactions. A high CPI value of 66 mN/m was also obtained for TP10. However, the extrapolation of the surface pressure for

$\pi i=0$ was similar to the π_{sat} (20 mN/m), suggesting that the peptide/lipid interaction was weaker than for M918 (Fig. 5). MAP and EB1 were able to insert into the phospholipids monolayer, with CPI values which are quite close to those previously measured for MPG, MPG-α, Pep-1 and CADY (Table 3). Nevertheless, the $\Delta\pi$ value for EB1 at $\pi i=0$ is 2,5 fold higher than its π_{sat}, suggesting stronger peptide/lipid interaction than in the case of MAP ($\Delta\pi=\pi_{sat}$ for $\pi i=0$). Taken together, these results indicate that all the peptides strongly interact with the charged phospholipids DOPG with the following order of interaction M918>TP10>EB1>MAP, but their interaction with neutral phospholipids is limited. Finally, the different results (CPI and $\Delta\pi$ for $\pi i=0$) obtained for the penetration experiments in the presence of DOPC and DOPG monolayer indicate slightly distinct behavior between the tested peptides. The CPI values for TP10, MAP, M918 and EB1 are higher in DOPG than in DOPC, indicating that strong electrostatic effect could affect their insertion into the lipid monolayer. This electrostatic effect seems to be more pronounced for M918.

In order to assess the consequence of CPP/membrane interactions on membrane stability, we have carried out leakage tests by following dye-release from pre-loaded LUVs. Results reported in Table 4, revealed that several of the peptides, identified as being able to interact with membrane, also induce leakage. The net increase (70%) of the ANTS fluorescence observed in the presence of MAP, suggests a strong membrane disruption and confirms its bilayer insertion and membrane-destabilizing activity as already reported (Table 4). CADY and EB1 induced a moderate leakage (30-40%) and ANTS leakage values obtained for TP10, M918, Penetratin and Tat (10%), reveal that these peptide have a poor tendency to destabilize membrane. Finally pVec and Arg9 did not induce any leakage, suggesting no membrane perturbation and probably no insertion into the liposome bilayer. That MAP, CADY, EB1 and to a certain extend TP10, and M918, are able to induced membranes destabilization, correlated with phospholipids monolayer penetration measurements,

supporting a net membrane insertion of MAP, CADY and EB1 and a less marked insertion for TP10 and M918.

4. Discussion

During the last two decades, cell-penetrating peptides have become promising tools for the intracellular delivery of therapeutics [31]. These peptide-carriers were developed in the beginning to cross the plasma membrane and reach the nucleus. Today, the number of optimized CPPs is constantly increasing in the search of improved efficacy, intracellular routing and specific tissues targeting. CPPs can be subdivided into two main classes, the first requiring chemical linkage with the cargo, and the second involving formation of stable, non-covalent complexes, which appears to be more appropriate for charged cargos such as siRNAs [1,39]. Although CPPs have been extensively used *in vitro*, *in vivo* and more recently at the clinical level, the mechanism by which they are able to deliver active cargoes inside the cell constitutes a complicated "brain-teaser" and remains the quest to the "Holy grail". In numerous cases, the cellular uptake the CPPs and the cargo-related biological response cannot be fully explained by endosomal routes triggered or not by electrostatic interactions with cell surface proteoglycans. Recently, structural properties and the ability of CPPs to interact with the lipid phase of the membrane have been reported to play a major role in the cellular uptake mechanism and the mode of action of CPPs. Comparative analysis of CPPs which have been reported so far, were focused on the delivery of covalently linked fluorophores [40] or biologically relevant cargo [41]. In the present work, we report the first comparative study of the structural plasticity of 10 well-known CPPs and their ability to interact with phospholipid membranes. We showed that the interaction of CPP with the membrane involves mainly electrostatic interactions and triggers a conformational transition of the peptides from random coil to helical or beta forms. We demonstrate that CPPs can be classified into three subgroups

depending on their physico-chemical properties, which correspond to distinct internalization pathways already reported in the literature.

4.1. Structural plasticity of the CPPs: polymorphism vs. monomorphism

The identification of the folding properties of the CPPs is clearly a major step for the understanding of their mode of action and has revealed that CPPs can adopt specific conformations, which are essential for membrane interactions and internalization. Analysis of the conformation of CPPs in different lipid mimicking environments by circular dichroism has allowed their classification into three distinct subgroups (Table 2, Fig. 1). The "disordered" subgroup contains cationic peptides such as Tat and Arg_9, which are fully polymorphic and unable to adopt any specific secondary structure whatever the nature of their environment. Tat and Arg_9 display no structural changes and remain disordered in the presence of phospholipids as already reported by several groups [42,43]. Although the folding of Tat has been discussed in numerous work so far no specific conformation has been clearly identified [43,44]. The peptides TP10, MAP, EB1, MPG-α, CADY and Pep-1 form the "helical" subgroup characterized by structural transition from a random coil (polymorphic behavior) in a solution to α-helix (monomorphic structure) in the presence of phospholipids. In contrast to TP10 and EB1 for which no structural data have been reported so far, the secondary amphipathic α-helical structure of MAP peptide has already been observed in the presence of different media [45,46]. The identification of a α-helix conformation for TP10 and EB1 is in a perfect agreement with previously reported theoretical predictions. Amphipathic helix structure was predicted *in silico* for TP10 based on the fact that it derived from Mastoparan segment known to be an amphipathic α-helix [23,47]. The EB1 sequence was derived from Penetratin by substituting residues 1 and 4 to histidines and extending the *N*-terminus with six amino acids in order to promote a helical structure [18]. This "helix"

subgroup of CPPs can be extended to CADY [29], Pep-1 [26] and MPG-α [25] peptides which also undergo a helical structural change (Table 2). Although MPG-α and Pep-1 are able to fold partially into a helix at high concentrations in a solution, their α-ellipticity is dramatically increased in the presence of phospholipids or SDS [25,28]. The helical contributions involve few residues of the peptide, suggesting a specific localization of the helix inside the sequence. Although an amphipathic distribution can be considered for MAP [21], CADY [27], Pep-1 [28] and the mastoparan domain of TP10 (as reported in [23]), the constitution of a secondary amphipathic helix is less straightforward for EB1. In addition, peptides of the "helix" group undergo an increase of their helical content in the presence of negatively charged vesicles, suggesting helix association. This could be due to both amphipathic feature and electrostatic effects. Although the helical domains seem to involve few residues of the sequence, they might induce specific amino acids distribution leading to helix aggregation through intermolecular interactions.

Finally, the peptides pVEC, retro-pVEC, M918, M1073, Penetratin and MPG constitute the "sheet" subgroup characterized by a phospholipid-mediated conformational transition from a disordered state to a β-sheet structure. The structural state of Penetratin seems to be highly dependent on the experimental conditions including the nature of the lipids and the phospholipid polar heads, buffers, concentrations and the technique used [48,49]. The structural versatility of Penetratin from unfolded to a β-sheet structure has been reported in the presence of negatively charged phospholipids [48,50,51 and this work], and to a helical-structure in various environments [43,52-55]. Concerning MPG, several spectroscopic analyses reveal a predominantly β-sheet structure in the presence of lipids vesicles and membrane mimicking solvents [56].

4.2. Helical structure is associated with strong CPP-membrane interactions

We showed that several CPPs can adopt a specific secondary structure, which play a major role in stabilizing their interactions with membranes and promoting their cellular uptake. During the internalization process, whether at the cell surface or inside endosomal vesicles or specific intracellular compartments, CPP/lipid interactions take place. We demonstrate that only few CPPs exhibit a significant affinity for the hydrophobic/hydrophilic interface. Tat and Arg_9 cationic CPPs as well as Penetratin and pVEC exhibited no affinity for the air-water interface for all the conditions and concentrations used .However the lack of affinity for interface does not indicate a lack of interactions. Penetratin and Arg_9 peptides have been reported to interact with negatively charged phospholipids [57,58]. In contrast, TP10, MAP, EB1 and M918 are the most amphipathic peptides; they strongly interact with DOPG, but only peptides from the "helix" group (TP10, MAP and EB1) are able to insert spontaneously into DOPC lipid monolayer. The CPI values suggest that TP10, MAP, EB1 and M918 are able to spontaneously insert into biological membranes mainly throughout strong electrostatic interactions with the polar heads of lipids rather than hydrophobic contacts with the lipids. In addition, there is a direct impact of the secondary structure that modulates the amphipathicity and membrane interaction/insertion of the CPPs. Indeed, negatively charged vesicles induced peptides conformational changes that were stronger than for zwiterrionic liposomes. This behavior highlights the importance of electrostatic interactions as already described for other peptides such as $S4_{13}$-PV [59]. Structural analyses of the peptide/lipid interactions indicate that peptides adopting a β-structure, such as M918 and MPG, are more sensitive to charges than the helical ones. Such a behavior differs from other CPPs for which a combination of electrostatic and hydrophobic interactions was identified. Indeed, for Pep-1 and CADY, the interactions with the lipids involved both electrostatic and hydrophobic contributions [28,29]. Thus helical peptides, such as TP10, EB1, MAP - and by extension

MPG-α, Pep-1 and CADY - seem to have a higher potential for peptide/lipids interactions, than β-structured MPG and M918 peptides.

Finally two additional points have to be considered: membrane stability and the location of the peptide within the membrane. Membrane leakage investigation has revealed that CPPs, which able to insert into lipid monolayer and to adopt helical secondary structure, can induce a more or less pronounced membrane disruption. Although some of them consists in well defined secondary amphipathic peptide (MAP, CADY and TP10), it seems that the observed membrane perturbation can not be clearly associated to the amphipathicity. Indeed EB1 that is less amphipathic than TP10 induces a better leakage. With regard to the peptide membrane insertion, although monolayer approaches seem to support an embedded location of carriers in the membrane, none straightforward conclusion can be pronounced. Only orientated CD, neutron diffusion or ATR-infra-red spectroscopy could distinguish a quasi-horizontal planar orientation compared to a vertically or tilted insertion.

4.3. Does structural Versatility of CPP control/impact internalization pathway?

Nowadays, it is clearly admitted that the first step in the cellular entry of CPPs corresponds to electrostatic interaction with cell surface proteoglycans, even if its not a prerequisite for the cellular uptake. Interaction with GAG induces their clustering at the cell surface and triggers activation of intracellular signals/actin remodeling and cell entry throughout numerous distinct internalization pathways ranging from direct translocation to endocytotic processes [14,41,60]. Thus the second determinant step mainly consists of peptide/lipid interactions that can lead both to the induction of a specific endocytotic pathway or to a membrane perturbation. In this regard, a conformational change, as identified for “sheet” and “helix” peptides, can modulate peptides/lipids interactions. The strength of these interactions might then determine whether the peptides remain entrapped at the plasma

membrane or not; and then whether the peptides follow an endocytotic route or induce membrane disorganization with direct translocation. As already mentioned, whether at the plasma membrane or inside endosomal vesicles, the nature of peptide/lipid interactions will determine the intracellular future of CPPs.

It has been proposed that the cellular internalization of the peptides could differ depending on their amphipathicity and polycationic nature, [41] and that the sequence length and conformation have a more important role than the accumulation of positive charges [40]. Furthermore, the structural versatility has been described as an important factor to consider for the deciphering of the cellular uptake of CPPs [51,59,61]. The present work support the idea that the structural plasticity could have a crucial role since inducing a specific amino acids distribution through a conformational change. This spatial reorganization allows a new balance between hydrophobic and hydrophilic surfaces with a specific charges distribution all along the conformation. Therefore CPPs modified their apparent hydrophilic/hydrophobic domains depending on the environment and on the nature of their peptide/lipid interactions [47,51 and this work]. We believe that the analysis of biophysical aspects needs a step by step approach that begins by the identification of intrinsic properties of the peptides. We sum up the structural and interaction properties of the different CPPs and proposed a model to classify the peptides regarding to their intrinsic biophysical features and their main internalization pathways (Fig. 6). The versatility of some CPPs should lead to both direct translocation and endocytotic process while the pronounced polymorphism of the others only induces an endocytotic mechanism. The strength and nature of peptide/lipids interactions will then determine the internalization mechanism.

Acknowledgments

This work was supported by the Centre National de la Recherche Scientifique (CNRS), the Agence Nationale de la Recherche (ANR), the Swedish Research Council (VR-NT), the Center for Biomembrane Research, Stockholm, and the Knut and Alice Wallenberg's Foundation. We thank Dr. Fatouma Said Hassane and Dr. Prisca Boisguerin for their precious help with leakage experiments. We thank Dr. May Catherine Morris (CRBM-UMR5237-CNRS) for critical reading of the manuscript and all members of the laboratory and our collaborators for fruitful discussions.

References

[1] F. Heitz, M.C. Morris, G. Divita, Twenty years of cell-penetrating peptides: from molecular mechanisms to therapeutics, Br. J. Pharmacol. 157 (2009) 195-206.

[2] Ü. Langel, Preface, Cell-Penetrating Peptides, 2nd edition, (Eds.: Ü. Langel), CRC Press, Boca Raton, (2007).

[3] G.P. Dietz, M. Bähr, Delivery of bioactive molecules into the cell: the Trojan horse approach, Mol. Cell. Neurosci. 27 (2004) 85-131.

[4] R. Fischer, M. Fotin-Mleczek, H. Hufnagel, R. Brock, Break on through to the other side-biophysics and cell biology shed light on cell-penetrating peptides, 6 Chembiochem. (2005) 2126-2142.

[5] D. Derossi, S. Calvet, A. Trembleau, A. Brunissen, G. Chassaing, A. Prochiantz, Cell internalization of the third helix of the Antennapedia homeodomain is receptor-independent, J. Biol. Chem. 271 (1996) 18188-18193.

[6] H. Binder, G. Lindblom, Charge-dependent translocation of the Trojan peptide penetratin across lipid membranes, Biophys. J. 85 (2003) 982-995.

[7] M.C. Morris, S. Deshayes, F. Heitz, G. Divita, Cell-penetrating peptides: from molecular mechanisms to therapeutics, Biol. Cell. 100 (2008) 201-217.

[8] M. Mano, C. Teodósio, A. Paiva, S. Simões, M.C. Pedroso de Lima, On the mechanisms of the internalization of S4(13)-PV cell-penetrating peptide, Biochem. J. 390 (2005) 603-612.

[9] I.M. Kaplan, J.S. Wadia, S.F. Dowdy, Cationic Tat peptide transduction domain enters cells by macropinocytosis, J. Control Release 102 (2005) 247-253.

[10] J.P. Richard, K. Melikov, H. Brooks, P. Prevot, B. Lebleu, L.V. Chernomordik, Cellular uptake of unconjugated TAT peptide involves clathrin dependent endocytosis and heparan sulfate receptors, J. Biol. Chem. 280 (2005) 15300-15306.

[11] A. Fittipaldi, A. Ferrari, M. Zoppe, C. Arcangeli, V. Pellegrini, F. Beltram, M. Giacca, Cell membrane lipid rafts mediate caveolar endocytosis of HIV-1 Tat fusion proteins, J. Biol. Chem. 278 (2003) 34141-34149.

[12] F. Duchardt, M. Fotin-Mleczek, H. Schwarz, R. Fischer, R. Brock, A comprehensive model for the cellular uptake of cationic cell-penetrating peptides, Traffic 8 (2007) 848-866.

[13] K. Padari, P. Säälik, M. Hansen, K. Koppel, R. Raid, Ü. Langel, M. Pooga, Cell transduction pathways of transportans, Bioconjug. Chem. 16 (2005) 1399-1410.

[14] G.M. Poon, J. Gariépy, Cell-surface proteoglycans as molecular portals for cationic peptide and polymer entry into cells, Biochem. Soc. Trans. 35 (2007) 788-793.

[15] P. Säälik, K. Padari, A. Niinep, A. Lorents, M. Hansen, E. Jokitalo, Ü. Langel, M. Pooga, Protein delivery with transportans is mediated by caveolae rather than flotillin-dependent pathways, Bioconjug. Chem. (2009) in press.

[16] S. Fawell, J. Seery, Y. Daikh, C. Moore, L.L. Chen, B. Pepinsky, J. Barsoum, Tat-mediated delivery of heterologous proteins into cells, Proc. Natl. Acad. Sci. U.S.A. 91 (1994) 664-668.

[17] D. Derossi, A.H. Joliot, G. Chassaing, A. Prochiantz, The third helix of the Antennapedia homeodomain translocates through biological membranes, J. Biol. Chem. 269 (1994) 10444-10450.

[18] P. Lundberg, S. El Andaloussi, T. Sütlü, H. Johansson, Ü. Langel, Delivery of short interfering RNA using endosomolytic cell-penetrating peptides, FASEB J. 21 (2007) 2664-2671.

[19] A. Elmquist, M. Lindgren, T. Bartfai, Ü. Langel, VE-cadherin-derived cell-penetrating peptide, pVEC, with carrier functions, Exp. Cell Res. 269 (2001) 237-244.

[20] S. El Andaloussi, H.J. Johansson, T. Holm, Ü. Langel, A novel cell-penetrating peptide, M918, for efficient delivery of proteins and peptide nucleic acids, Mol. Ther. 15 (2007) 1820-1826.

[21] J. Oehlke, A. Scheller, B. Wiesner, E. Krause, M. Beyermann, E. Klauschenz, M. Melzig, M. Bienert, Cellular uptake of an alpha-helical amphipathic model peptide with the potential to deliver polar compounds into the cell interior non-endocytically, Biochim. Biophys. Acta 1414 (1998) 127-139.

[22] P.A. Wender, D.J. Mitchell, K. Pattabiraman, E.T. Pelkey, L. Steinman, J.B. Rothbard, The design, synthesis, and evaluation of molecules that enable or enhance cellular uptake: peptoid molecular transporters, Proc. Natl. Acad. Sci. U.S.A. 97 (2000) 13003-13008.

[23] U. Soomets, M. Lindgren, X. Gallet, M. Hällbrink, A. Elmquist, L. Balaspiri, M. Zorko, M. Pooga, R. Brasseur, Ü. Langel, Deletion analogues of transportan, Biochim. Biophys. Acta. 1467 (2000) 165-176.

[24] M.C. Morris, P. Vidal, L. Chaloin, F. Heitz, G. Divita, A new peptide vector for efficient delivery of oligonucleotides into mammalian cells, Nucleic Acids Res. 25 (1997) 2730-2736.

[25] S. Deshayes, T. Plénat, G. Aldrian-Herrada, G. Divita, C. Le Grimellec, F. Heitz, Primary amphipathic cell-penetrating peptides: structural requirements and interactions with model membranes, Biochemistry 43 (2004) 7698-7706.

[26] M.C. Morris, J. Depollier, J. Mery, F. Heitz, G. Divita, A peptide carrier for the delivery of biologically active proteins into mammalian cells, Nat. Biotechnol. (2001) 19 1173-1176.

[27] L. Crombez, G. Aldrian-Herrada, K. Konate, Q.N. Nguyen, G.K. McMaster, R. Brasseur, F. Heitz, G. Divita, A new potent secondary amphipathic cell-penetrating peptide for siRNA delivery into mammalian cells, Mol. Ther. 17 (2009) 95-103.

[28] S. Deshayes, A. Heitz, M.C. Morris, P. Charnet, G. Divita, F. Heitz, Insight into the mechanism of internalization of the cell-penetrating carrier peptide Pep-1 through conformational analysis, Biochemistry 43 (2004) 1449-1457.

[29] K. Konate, L. Crombez, S. Deshayes, A. Thomas, R. Brasseur, G. Aldrian-Herrada, F. Heitz, G. Divita, Insight into the cellular uptake mechanism of a secondary amphipathic cell penetrating peptide for siRNA delivery, Biochemistry (2010) in press.

[30] R. Maget-Dana, The monolayer technique: a potent tool for studying the interfacial properties of antimicrobial and membrane-lytic peptides and their interactions with lipid membranes. Biochim. Biophys. Acta 1462 (1999) 109-140.

[31] S. Deshayes, M.C. Morris, G. Divita, F. Heitz, Cell-penetrating peptides: tools for intracellular delivery of therapeutics, Cell. Mol. Life Sci. 62 (2005) 1839-1849.

[32] N. Greenfield, G.D. Fasman, Computed circular dichroism spectra for the evaluation of protein conformation, Biochemistry 8 (1969) 4108-4116.

[33] S.Y.M. Lau, A.K. Taneja, R.S. Hodges, Synthesis of a model protein of defined secondary and quaternary structure. Effect of chain length on the stabilization and formation of two-stranded α-helical coiled-coils, J. Biol. Chem. 259 (1984) 13253-13261.

[34] C. McNamara, A.S. Zinkernagel, P. Macheboeuf, M.W. Cunningham, V. Nizet, P. Ghosh, Coiled-coil irregularities and instabilities in group A Streptococcus M1 are required for virulence, Science, 319 (2008) 1405-1408.

[35] H. Brockman, Lipid monolayers: why use half a membrane to characterize protein-membrane interactions? Curr. Opin. Struct. Biol. 9 (1999) 438-443.

[36] P. Calvez, S. Bussières, E. Demers, C. Salesse, Parameters modulating the maximum insertion pressure of proteins and peptides in lipid monolayers, Biochimie 91 (2009) 718-733.

[37] M. Rafalski, J.D. Lear, W.F. DeGrado, Phospholipid interactions of synthetic peptides representing the N-terminus of HIV gp41, Biochemistry 29 (1990) 7917-7922.

[38] R.A. Demel, W.S. Geurts van Kessel, R.F. Zwaal, B. Roelofsen, L.L. van Deenen, Relation between various phospholipase actions on human red cell membranes and the interfacial phospholipid pressure in monolayers, Biochim. Biophys. Acta 406 (1975) 97-107.

[39] B.R. Meade, S.F. Dowdy, Enhancing the cellular uptake of siRNA duplexes following noncovalent packaging with protein transduction domain peptides, Adv. Drug Deliv. Rev. 60 (2008) 530-536.

[40] J. Mueller, I. Kretzschmar, R. Volkmer, P. Boisguerin, Comparison of cellular uptake using 22 CPPs in 4 different cell lines, Bioconjug. Chem. 19 (2008) 2363-2374.

[41] P. Lundin, H. Johansson, P. Guterstam, T. Holm, M. Hansen, Ü. Langel, S. El Andaloussi, Distinct uptake routes of cell-penetrating peptide conjugates, Bioconjug. Chem. 19 (2008) 2535-2542.

[42] M. Law, M. Jafari, P. Chen, Physicochemical characterization of siRNA-peptide complexes, Biotechnol. Prog. 24 (2008) 957-963.

[43] M. Orzáez, L. Mondragón, I. Marzo, G. Sanclimens, A. Messeguer, E. Pérez-Payá, M.J. Vicent, Conjugation of a novel Apaf-1 inhibitor to peptide-based cell-membrane transporters:

effective methods to improve inhibition of mitochondria-mediated apoptosis, Peptides 28 (2007) 958-968.

[44] P. Ruzza, A. Calderan, A. Guiotto, A. Osler, G. Borin, Tat cell-penetrating peptide has the characteristics of a poly(proline) II helix in aqueous solution and in SDS micelles, J. Pept. Sci. 10 (2004) 423-426.

[45] M. Dathe, M. Schürmann, T. Wieprecht, A. Winkler, M. Beyermann, E. Krause, K. Matsuzaki, O. Murase, M. Bienert, Peptide helicity and membrane surface charge modulate the balance of electrostatic and hydrophobic interactions with lipid bilayers and biological membranes, Biochemistry 35 (1996) 12612-12622.

[46] J. Bürck, S. Roth, P. Wadhwani, S. Afonin, N. Kanithasen, E. Strandberg, A.S.Ulrich, Conformation and membrane orientation of amphiphilic helical peptides by oriented circular dichroism, Biophys. J. 95 (2008) 3872-3881.

[47] S. Deshayes, M. Decaffmeyer, R. Brasseur, A. Thomas, Structural polymorphism of two CPP: an important parameter of activity, Biochim. Biophys. Acta 1778 (2008) 1197-1205.

[48] M. Magzoub, L.E. Eriksson, A. Gräslund, Conformational states of the cell-penetrating peptide penetratin when interacting with phospholipid vesicles: effects of surface charge and peptide concentration, Biochim. Biophys. Acta. 1563 (2002) 53-63.

[49] M. Magzoub, L.E. Eriksson, A. Gräslund, Comparison of the interaction, positioning, structure induction and membrane perturbation of cell-penetrating peptides and non-translocating variants with phospholipid vesicles, Biophys. Chem. 103 (2003) 271-288.

[50] M. Magzoub, K. Kilk, L.E. Eriksson, Ü. Langel, A. Gräslund, Interaction and structure induction of cell-penetrating peptides in the presence of phospholipid vesicles, Biochim. Biophys. Acta 1512 (2001) 77-89.

[51] Y. Su, R. Mani, T. Doherty, A.J. Waring, M. Hong, Reversible sheet-turn conformational change of a cell-penetrating peptide in lipid bilayers studied by solid-state NMR, J. Mol. Biol. 381 (2008) 1133-1144.

[52] W.L. Zhu, S.Y. Shin, Antimicrobial and cytolytic activities and plausible mode of bactericidal action of the cell penetrating peptide penetratin and its lys-linked two-stranded peptide, Chem. Biol. Drug Des. 73 (2009) 209-215.

[53] A.A. Polyansky, P.E. Volynsky, A.S. Arseniev, RG. Efremov, Adaptation of a Membrane-active Peptide to Heterogeneous Environment. I. Structural Plasticity of the Peptide, J. Phys. Chem. B. 113 (2009) 1107-1119.

[54] I.D. Alves, N. Goasdoue, I. Correia, S. Aubry, C. Galanth, S. Sagan, S. Lavielle, G. Chassaing, Membrane interaction and perturbation mechanisms induced by two cationic cell penetrating peptides with distinct charge distribution, Biochim Biophys Acta 1780 (2008) 948-959.

[55] S. Balayssac, F. Burlina, O. Convert, G. Bolbach, G. Chassaing, O. Lequin, Comparison of penetratin and other homeodomain-derived cell-penetrating peptides: interaction in a membrane-mimicking environment and cellular uptake efficiency, Biochemistry 45 (2006) 1408-20.

[56] S. Deshayes, S. Gerbal-Chaloin, M.C. Morris, G. Aldrian-Herrada, P. Charnet, G. Divita, F. Heitz, On the mechanism of non-endosomial peptide-mediated cellular delivery of nucleic acids, Biochim. Biophys. Acta 1667 (2004) 141-147.

[57] D. Terrone, S.L. Sang, L. Roudaia, J.R. Silvius, Penetratin and related cell-penetrating cationic peptides can translocate across lipid bilayers in the presence of a transbilayer potential, Biochemistry 42 (2003) 13787-13799.

[58] H.L. Lee, E.A. Dubikovskaya, H. Hwang, A.N. Semyonov, H. Wang, L.R. Jones, R.J. Twieg, W.E. Moerner, P.A. Wender, Single-molecule motions of oligoarginine transporter

conjugates on the plasma membrane of Chinese hamster ovary cells, J. Am. Chem. Soc. 130 (2008) 9364-9370.

[59] M. Mano, A. Henriques, A. Paiva, M. Prieto, F. Gavilanes, S. Simões, M.C. Pedroso de Lima, Interaction of S413-PV cell penetrating peptide with model membranes: relevance to peptide translocation across biological membranes, J. Pept. Sci. 13 (2007) 301-313.

[60] A. Ziegler, J. Seelig, Binding and clustering of glycosaminoglycans: a common property of mono- and multivalent cell-penetrating compounds, Biophys. J. 94 (2008) 2142-2149.

[61] C. El Amri, P. Nicolas, Plasticins: membrane-damaging peptides with “chameleon-like” properties, Cell. Mol. Life Sci. 65 (2008) 895-909.

Tables

Table 1. Sequences of the CPPs

Origin	Name	Sequence	aa	MW [Da]	Ref.
Protein Transduction Domain (PTD)	Tat	GRKKRRQRRRPPQ-NH_2	13	1718.1	[16]
	Penetratin	RQIKIWFQNRRMKWKK-NH_2	16	2245.1	[17]
	EB1	LIRLWSHLIHIWFQNRRLKWKKK-NH_2	23	3099.8	[18]
	pVEC	LLIILRRRIRKQAHAHSK-NH_2	18	2208.8	[19]
	Retro-pVEC	KSHAHAQKRIRRRLIILL-NH_2	18	2208.8	[19]
	M918	MVTVLFRRLRIRRACGPPRVRV-NH_2	22	2651.4	[20]
	M1073	MVTVLFRRLRIRRASGPPRVRV-NH_2	22	2635.3	[20]
Model Peptides	MAP	KLALKLALKALKAALKLA-NH_2	18	1876.5	[21]
	Arg_9	RRRRRRRRR-NH_2	9	1422.8	[22]
Designed Peptides	TP10	AGYLLGKINLKALAALAKKIL-NH_2	21	2181.8	[23]
	MPG	GALFLGFLGAAGSTMGAWSQPKKKRKV-Cya	27	2908.5	[24]
	MPG-α	GALFLAFLAAALSLMGLWSQPKKKRKV-Cya	27	3047.0	[25]
	Pep-1	KETWWETWWTEWSQPKKKRKV-Cya	21	2907.4	[26]
	CADY	GLWRALWRLLRSLWRLLWKA-Cya	20	2653.0	[27]

Table 2. Structural Characterization of the CPPs

Peptide	Structure * (Water)	Structure * (DOPG)	Structure * (DOPC/DOPG)	Structure * (DOPC)	Structure * (DOPC/SM/Chol)	Ref.
YDEGE (control)	rc	rc	rc	rc	rc	-
Tat	rc	rc	rc	rc	rc	-
Arg_9	rc	rc	rc	rc	rc	-
pVEC	rc	β-strand / rc	rc	rc	rc	-
Retro-pVEC	rc	β-strand / rc	rc	rc	rc	-
Penetratin	rc	β-strand / rc	rc	rc	rc	-
M918	rc	β-strand	rc	rc	rc	-
M1073	rc	β-strand	rc	rc	rc	-
TP10	rc	α-Helix	α-Helix / rc	rc	rc	-
MAP	rc	α-Helix	α-Helix / rc	rc	rc	-
EB1	rc	α-Helix	α-Helix / rc	rc	rc	-
MPG	rc	β-strand / rc	β-strand / rc	nd	nd	[25,55]
MPG-α	rc	α-Helix / rc	α-Helix / rc	nd	nd	[25]
Pep-1	rc and α-Helix at high concentration	α-Helix / rc	α-Helix / rc	nd	α-Helix / rc	[28]
CADY	rc	α-Helix	α-Helix	α-Helix / rc	α-Helix	[27,29]

* : The main secondary structure is reported

rc : random coil

nd : not determined

Table 3. CMC and CPI of the CPPs

Peptide	CMC (nM)	Saturating pressure π_{sat} (mN/m)	CPI in DOPG (mN/m)	CPI in DOPC (mN/m)	Ref.
TP10	38	20	66	31	-
MAP	59	14	40	28	-
EB1	91	10	54	33	-
M918	130	7	78	23	-
Arg_9	*	*	nd	nd	-
Tat	*	*	nd	nd	-
Penetratin	*	*	nd	nd	-
pVEC	*	*	nd	nd	-
MPG	250	13	48	33	[25]
MPG-α	400	25	39	33	[25]
Pep-1	500	5	*45*	*45*	[28]
CADY	230	30	*43*	*43*	[29]

CMC : Critical micellar concentration

CPI : Critical pressure of insertion

* : No significant increase in the surface pressure, even at 1µM

nd : not determined

Table 4. Leakage of liposomes induced by CPPs monitored by fluorescence spectroscopy. The peptide concentration used is 1µM and the lipid/peptide molar ratio is 40/1.

Peptides	% of leakage after 15 min
MAP	70
CADY	38
EB1	26
TP10	12
M918	12
Penetratin	9
Tat	8
pVec	2
Arg9	1

Legends of figures

Figure 1: Conformational analysis of CPPs by circular dichroism spectroscopy. The peptides were tested in their free form and in the presence of different amounts of negatively charged DOPG phospholipid vesicles. The peptides are classified into three subgroups: (A) the non-ordered peptides such as Tat, (B) the "sheet" peptides such as M918 and (C) the "helix" peptides such as EB1. CD spectra are recorded for peptides at 75µM in their free form (black) and in the presence of pure DOPG vesicles at 1/1 (blue), 2/1 (red), 5/1 (green) and 10/1 (grey) lipid/peptide ratios. Mean molar ellipticity per residues is expressed in $deg.cm^2.dmol^{-1}$.

Figure 2: Structural state of TP10 in various environments. Circular dichroism spectra were recorded for TP10 at 75µM in its free form and in the presence of pure zwiterrionic DOPC SUVs (A), mixture of DOPC/DOPG at an 80/20 ratio (B), pure negatively charged DOPG SUVs (C) and DOPC/SM/Chol LUVs (D). CD spectra correspond to pure peptide (black) and peptide in the presence of lipid vesicles at 2/1 (blue), 5/1 (red), 10/1 (green) and 20/1 (grey) lipid/peptide ratios for DOPC, DOPC/DOPG and DOPC/SM/Chol vesicles and at 1/1 (blue), 2/1 (red), 5/1 (green) and 10/1 (grey) lipid/peptide ratios for DOPG. Mean molar ellipticity per residues is expressed in $deg.cm^2.dmol^{-1}$.

Figure 3: Peptide-induced variations of the surface pressures as a function of peptide concentrations in the subphase. TP10 (1), MAP (2), EB1 (3) constituted the "helix" peptides subgroups while M918 (4), pVEC (5) and Penetratin (6) the "sheet" subgroup, and Arg_9 (7) and Tat (8) belong to the "disordered" subgroup. No variations of the surface pressure are detected for Penetratin, Arg_9 and Tat.

Figure 4: Insertion of MAP, TP10, M918 and EB1 into DOPC monolayers. The surface pressure variations induced by TP10 (■), MAP (□), EB1 (●) and M918 (○) are reported as a function of the initial pressure of the DOPC monolayer. Extrapolation at zero pressure variation ($\Delta\pi=0$) gives the critical pressure of insertion (CPI).

Figure 5: Insertion of MAP, TP10, M918 and EB1 into DOPG monolayers. The surface pressure variations induced by TP10 (■), MAP (□), EB1 (●) and M918 (○) are reported as a function of the initial pressure of the DOPG monolayer. Extrapolation at zero pressure variation ($\Delta\pi=0$) gives the critical pressure of insertion (CPI).

Figure 6: A model of different lipid interaction abilities of CPPs and their associated internalization pathways.

Figure 1

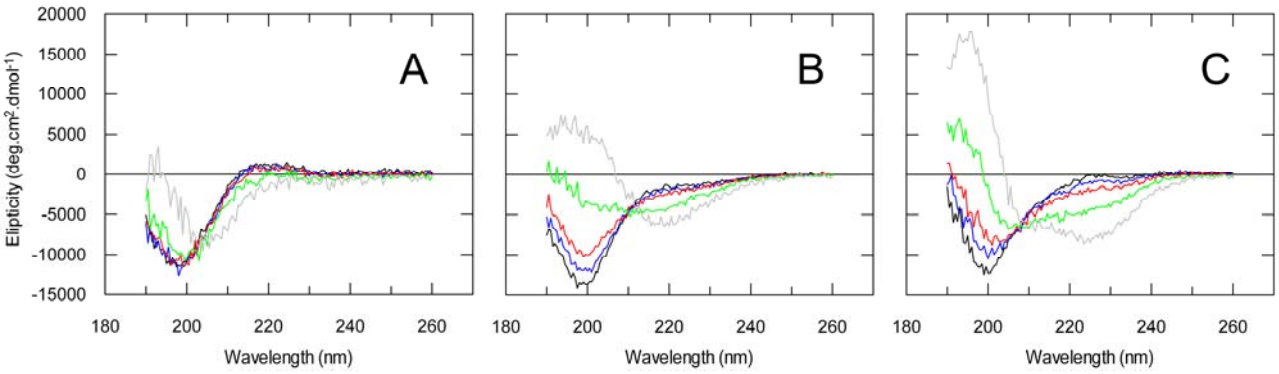
A
B
C
Elipticity (deg.cm².dmol⁻¹)
20000
15000
10000
5000
0
-5000
-10000
-15000
180
200
220
240
260
Wavelength (nm)

Figure 2

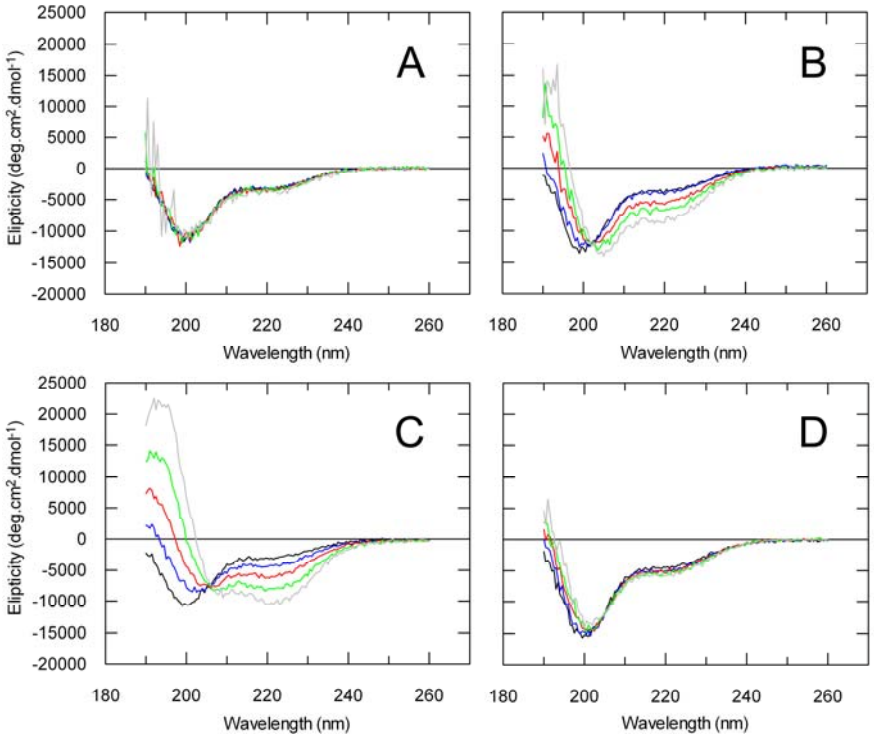
A
B
C
D
Elipticity (deg.cm².dmol⁻¹)
Wavelength (nm)
25000
20000
15000
10000
5000
0
-5000
-10000
-15000
-20000
180
200
220
240
260

Figure 3

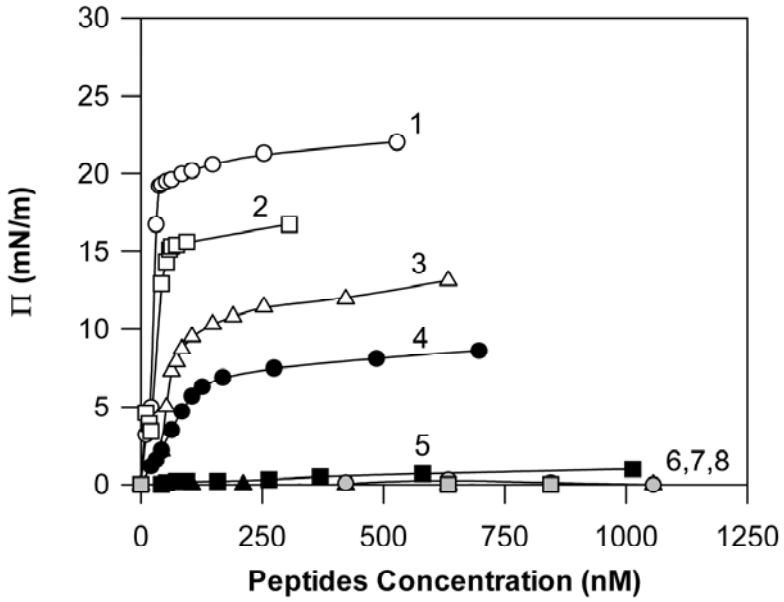
30
25
20
15
10
5
0
Π (mN/m)
1
2
3
4
5
6,7,8
0
250
500
750
1000
1250
Peptides Concentration (nM)

Figure 4

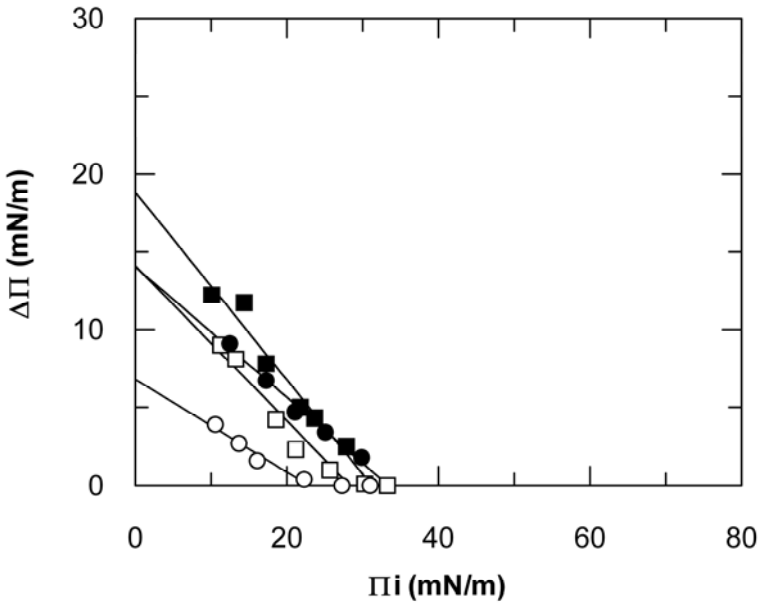

Figure 5

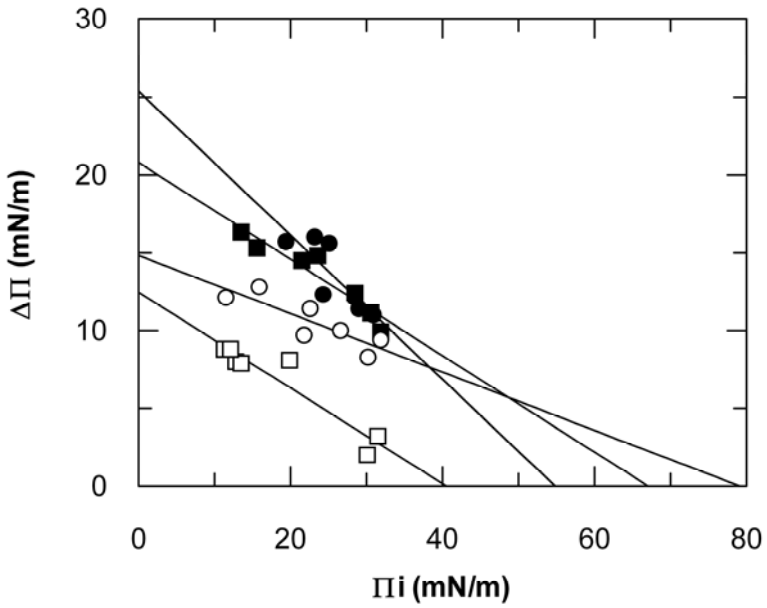

Figure 6

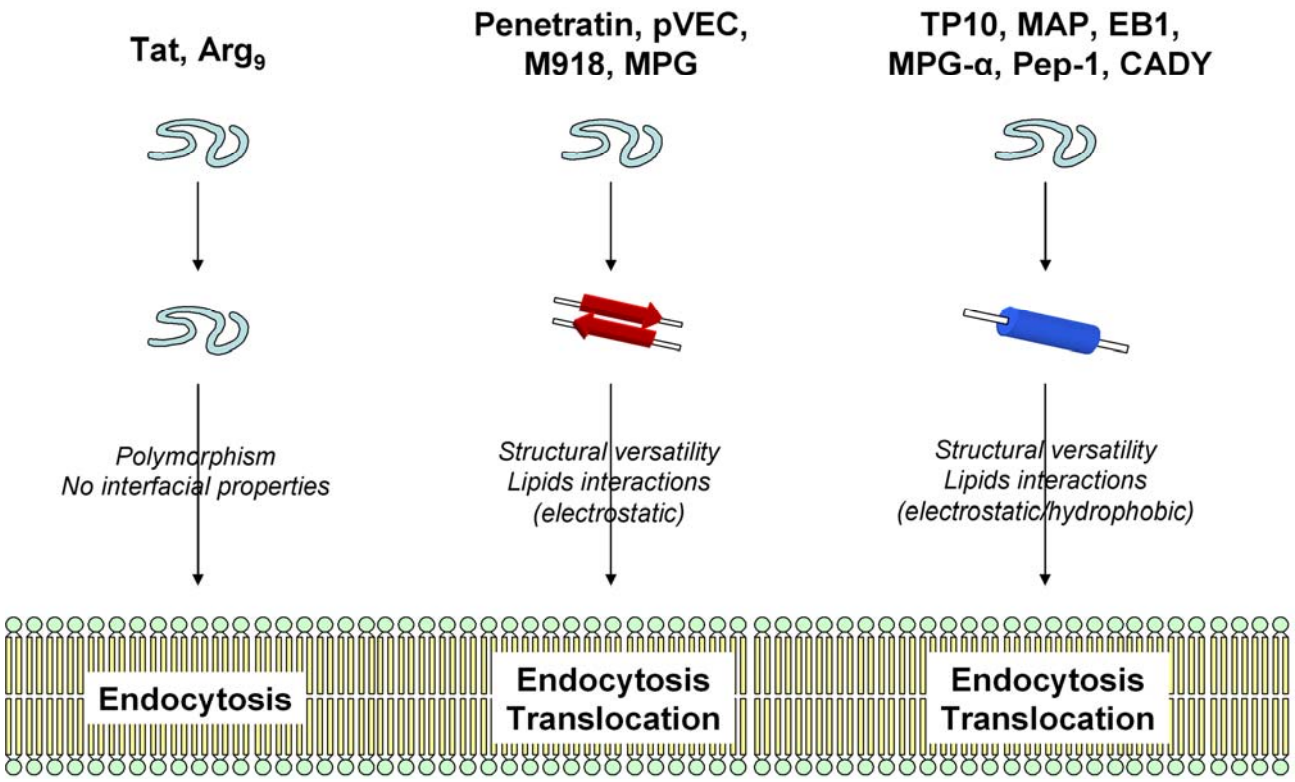
Tat, Arg9
Penetratin, pVEC, M918, MPG
TP10, MAP, EB1, MPG-α, Pep-1, CADY
Polymorphism
No interfacial properties
Structural versatility
Lipids interactions
(electrostatic)
Structural versatility
Lipids interactions
(electrostatic/hydrophobic)
Endocytosis
Endocytosis Translocation
Endocytosis Translocation